ORIGINAL ARTICLE

AXL is required for hypoxia-mediated hypoxia-inducible factor-1 alpha function in glioblastoma

Thuy-Trang T. Vo[1,2] · Quangdon Tran[1,2] · Youngeun Hong[1,2] · Hyunji Lee[1,2] · Hyeonjeong Cho[1,2] · Minhee Kim[1,2] · Sungjin Park[1,2] · Chaeyeong Kim[1,2] · Choinyam Bayarmunkh[3,4] · Damdindorj Boldbaatar[3,4] · So Hee Kwon[5] · Jisoo Park[1,2,6] · Seon-Hwan Kim[7] · Jongsun Park[1,2]

Abstract

Glioblastoma (GBM) is the most aggressive type of central nervous system tumor. Molecular targeting may be important when developing efficient GBM treatment strategies. Sequencing of GBMs revealed that the receptor tyrosine kinase (RTK)/RAS/phosphatidylinositol-3-kinase pathway was altered in 88% of samples. Interestingly, AXL, a member of RTK, was proposed as a promising target in glioma therapy. However, the molecular mechanism of AXL modulation of GBM genesis and proliferation is still unclear. In this study, we investigated the expression and localization of hypoxia-inducible factor-1 alpha (HIF-1α) by AXL in GBM. Both AXL mRNA and protein are overexpressed in GBM. Short-interfering RNA knockdown of AXL in U251-MG cells reduced viability and migration. However, serum withdrawal reduced AXL expression, abolishing the effect on viability. AXL is also involved in hypoxia regulation. In hypoxic conditions, the reduction of AXL decreased the level and nuclear localization of HIF-1α. The co-expression of HIF-1α and AXL was found in human GBM samples but not normal tissue. This finding suggests a mechanism for GBM proliferation and indicates that targeting AXL may be a potential GBM therapeutic.

Keywords AXL · Tyrosine kinase · Glioblastoma · Hypoxia · HIF-1α

Introduction

Malignant gliomas, including anaplastic astrocytomas and glioblastomas (GBM), are aggressive tumors that confer a poor prognosis [1–5]. Glioblastoma was the first cancer to be systematically analyzed by The Cancer Genome Atlas

Thuy Trang T. Vo, Quangdon Tran and Youngeun Hong equally contributed to this work.

✉ Seon-Hwan Kim
neons@cnu.ac.kr

✉ Jongsun Park
insulin@cnu.ac.kr

1 Department of Pharmacology, College of Medicine, Chungnam National University, Daejeon 35015, Republic of Korea

2 Department of Medical Science, Metabolic Syndrome and Cell Signaling Laboratory, Institute for Cancer Research, College of Medicine, Chungnam National University, Daejeon 35015, Republic of Korea

3 Department of Graduate Education, Graduate School, Mongolian National University of Medical Sciences, Ulaanbaatar 14210, Mongolia

4 Department of Physiology, Mongolian National University of Medical Sciences, Ulaanbaatar 14210, Mongolia

5 College of Pharmacy, Yonsei Institute of Pharmaceutical Sciences, Yonsei University, Incheon 21983, Republic of Korea

6 Department of Life Science, Hyehwa Liberal Arts College, LINC Plus Project Group, Daejeon University, Daejeon 34520, Republic of Korea

7 Department of Neurosurgery, Institute for Cancer Research, College of Medicine, Chungnam National University, Daejeon 35015, Republic of Korea

(TCGA) network [6, 7]. Sequencing of these tumors revealed that the receptor tyrosine kinase (RTK)/RAS/phosphatidylinositol-3-kinase (PI3K) pathway was altered in 88% of samples [6, 7]. Interestingly, a receptor tyrosine kinases (RTK), AXL displayed a promising target in glioma therapy in previous studies [8–10], and may modulate GBM genesis and proliferation.

AXL involved in the regulation of multiple aspects of tumorigenesis. Originally, AXL was cloned from patients with chronic myelogenous leukemia and it exhibited transforming potential when overexpressed [11]. AXL overexpression has been reported in a variety of human cancers [12–17]. The upregulation of AXL is associated with invasiveness and metastasis in lung [16], head and neck cancer [17], prostate [18], breast [19] and gastric cancers [20] as well as in renal cell carcinoma [21] and glioblastoma [9]. AXL overexpression via a 'tyrosine kinase switch' leads to resistance to imatinib in gastrointestinal stromal tumors [22]. AXL expression is induced by chemotherapy drugs and overexpression of AXL confers drug resistance in acute myeloid leukemia [23]. AXL was also suggested as a marker for the prediction of prognosis in several cancers [8, 24–26].

Hypoxia is known as a stimulus for angiogenesis, mainly via hypoxia-inducible factor-1 alpha (HIF-1α) [27, 29], which regulates the transcription of several genes mediating tumor responses to hypoxia such as tumor cell proliferation, survival, migration and angiogenesis [27, 29]. During tumor hypoxia, HIF-1α is a regulator of vascular endothelial growth factor (VEGF) and modulates angiogenesis by upregulating the VEGF gene [27, 28, 30]. Sustained angiogenesis is one of the hallmarks of cancer [31] and is a complex multi-step process essential for tumor growth, invasion and metastatic spread [27, 32, 33]. Interestingly, AXL has been identified as a direct HIF-1α target gene in breast and renal cancer. HIF-1α has been shown to act as a tumor suppressor, as elevated expression of HIF-1α reduces tumor size, while HIF-1α knockdown increases cell proliferation [34–37]. AXL, on the other hand, can promote the stabilization and activation of HIF-1α in hypoxic conditions, leading to increased expression of HIF-1α target genes. This occurs through several mechanisms, including promoting the translocation of HIF-1α to the nucleus and enhancing the activity of HIF-1α transcriptional activity. Conversely, HIF-1α can also regulate the expression of AXL. HIF-1α can induce the expression of AXL in hypoxic conditions, and this upregulation of AXL expression is thought to contribute to the invasive and metastatic behavior of cancer cells [34, 35, 37, 38]. This complex and bidirectional relationship between AXL and HIF-1α requires further research to fully understand the molecular mechanisms involved and their implications for cancer biology and therapy. In this study, we investigated the role of AXL in the expression and localization of HIF-1α in GBM. Our findings suggest that AXL plays a crucial role in promoting GBM proliferation, and targeting AXL expression may hold therapeutic potential for treating GBM. Overall, this study provides new insights into the intricate interplay between AXL and HIF-1α in cancer biology, and highlights the importance of investigating these relationships for developing effective cancer therapies.

Materials and methods

Antibodies and reagents

Anti-actin antibody was purchased from Sigma–Aldrich (St. Louis, MO, USA). Horseradish peroxidase-conjugated anti-mouse IgG or anti-rabbit IgG secondary antibodies were purchased from Komabiotech (Seoul, Korea), Anti-AXL antibody was purchased from Santa Cruz Biotechnology (Dallas, TX, USA).

Patient samples

The study was approved by the Hospital Institutional Review Board (approval number CNUH 2018-03-014) according to the Declaration of Helsinki at Chungnam National University Hospital (Daejeon, Korea). The biospecimens and data used for this study were provided by the Biobank of Chungnam National University Hospital, a member of the Korea Biobank Network.

Cell culture

The glioblastoma cells (U87-MG, U251-MG and U343-MG) were maintained in medium (RPMI) supplemented with 10% fetal bovine serum (FBS), 25 mM HEPES (Thermo Scientific, Waltham, MA, USA), 1% Antibiotics-Antimycotics (Life Technologies, Carlsbad, CA, USA).

Immunoblot analysis

The western blot analysis was performed as the previously described [39, 40]. Briefly, cells were placed on ice and extracted with lysis buffer containing 50 mM Tris–HCl, pH 7.5, 1% v/v Nonidet P-40, 120 mM NaCl, 25 mM sodium fluoride, 40 mM β-glycerol phosphate, 0.1 mM

sodium orthovanadate, 1 mM phenylmethylsulfonyl fluoride, 1 mM benzamidine, and 2 µM microcystin-LR. Lysates were centrifuged for 15 min at 12,000 g. The cell extracts were resolved by 10–15% SDS-PAGE, and transferred to Immobilon-P membranes (Millipore, Burlington, MA, USA). The filters were blocked for 1 h in 1 X tri-buffered saline buffer (TBS; 140 mM NaCl, 2.7 mM KCl, 250 mM Tris- HCl, pH 7.4), containing 5% skimmed milk and 0.2% Tween-20, followed by an overnight incubation with the anti-AXL and anti-actin antibodies diluted 1000-fold at 4 °C. The secondary antibody was horseradish peroxidase-conjugated anti-mouse IgG or anti-rabbit IgG (Komabiotech, Seoul, Korea), diluted 5000-fold in blocking buffer. The detection of protein expression was visualized by enhanced chemiluminescence, according to the manufacturer's instructions (Thermo Fisher Scientific).

Real-time quantitative reverse transcription-polymerase chain reaction (qRT-PCR)

Total RNAs were extracted from frozen tissue samples or from cells using the PureHelix RNA Extraction Solution (Nanohelix, Daejeon, South Korea). The cDNA was synthesized from total RNA with the SuperScript III First-Strand Synthesis System for qRT-PCR (Invitrogen, Grand Island, NY, USA). The qRT-PCR measurement of individual cDNAs was performed using SYBR green dye to measure duplex DNA formation with the StepOne Plus real-time PCR system (Invitrogen) and normalized to the expression of glyceraldehyde 3-phosphate dehydrogenase (*GAPDH*) RNA. The following primers were used in the qRT-PCR (F: Forward, R: Reverse); Human *AXL*: F-5'-GTCCTCATC TTGGCTCTCTTC / R-5'- GACTACCA GTTCACCTCTT-TCC; human *GAPDH*: F-5'-TCGACAGTCAGCCGCATC TTCTTT / R-5'-TACGACCA AATCCGTTGACTCCGA.

Real-time assay for cell proliferation and migration

Real-time assay for cell proliferation and migration were measured using an xCELLigence RTCA DP system (Roche Applied Science, Indianapolis, IN, USA), which monitors cellular events in real-time without the incorporation of labels. Briefy, cells were placed into well of an E-plate 16 (for proliferation; U251-MG, 3×10^3 cells) and incubated for indicated times.

RNA sequencing and RNA-Seq data analysis

Total RNA of U87-MG cell, U251-MG cell and normal brain was extracted using Trizol reagent (Invitrogen) following the manufacturer's procedures. The total RNA quantity and purity were analysis of Bioanalyzer 2100 and RNA 6000 Nano LabChip Kit (Agilent, Santa Clara, CA, USA). Roughly 10 µg of total RNA was used to isolate poly(A) mRNA with poly(T) oligo-attached magnetic beads (Invitrogen). Following purification, the mRNA is fragmented into small pieces using divalent cations under increased temperature. Next, the cleaved RNA fragments were reverse-transcribed to create the final cDNA library in accordance with the protocol for the mRNA-Seq sample preparation kit (Illumina, San Diego, CA, USA). The average insert size for the paired-end libraries was 300 bp (± 50 bp). Next we performed the paired-end sequencing on an Illumina Hiseq 2000 system at Macrogen (Seoul, Korea) following the vendor's instructions. For each sample, sequenced reads were aligned to the UCSC human reference genome (http://ccb. jhu.edu/software/tophat) using the Tophat package (http://genome.ucsc.edu/), which initially removes a portion of the reads based on quality information accompanying each read and then maps the reads to the reference genome. Fragments per kilobase of exon per million fragments mapped (FPKM) were calculated to compare the expression level of *AXL* mRNA variants in each sample.

Confocal imaging analysis and indirect immunofluorescence

U251-MG cells were grown on glass coverslips and transfected with plasmids. After 24 h, the cells were fixed in 4% paraformaldehyde at room temperature for 10 min and permeabilized in 0.2% Triton ×100 for 5 min at room temperature. Then cells were incubated in blocking buffer containing 5% bovine serum albumin (Sigma–Aldrich, St. Louis, MO, USA) in 1× TBS for 1 h at 37 °C. The rabbit polyclonal anti-AXL antibody was diluted 200-fold and incubated overnight. FITC-conjugated anti-rabbit antibody (BD Biosciences, San Jose, CA, USA) was used as the secondary antibody. After appropriate rinsing, coverslips were mounted with Vectashield (Vector Laboratories, Burlingame, CA, USA) and visualized using a Zeiss confocal microscope.

Immunohistochemistry

The immunohistochemistry analysis was performed as previously described [41]. A human cancer tissue array slide with paraffin sections was purchased from US Biomax Inc. (Derwood, MD, USA). Histostain-Plus kits (Zymed Laboratories Inc., South San Francisco, CA, USA) were used following the manufacturer's instructions for immunohistochemistry of the tissue array. Briefly, paraffin sections were deparaffinized with xylene and rehydrated in a graded series of ethanol. The slide was submerged in peroxidase quenching solution for
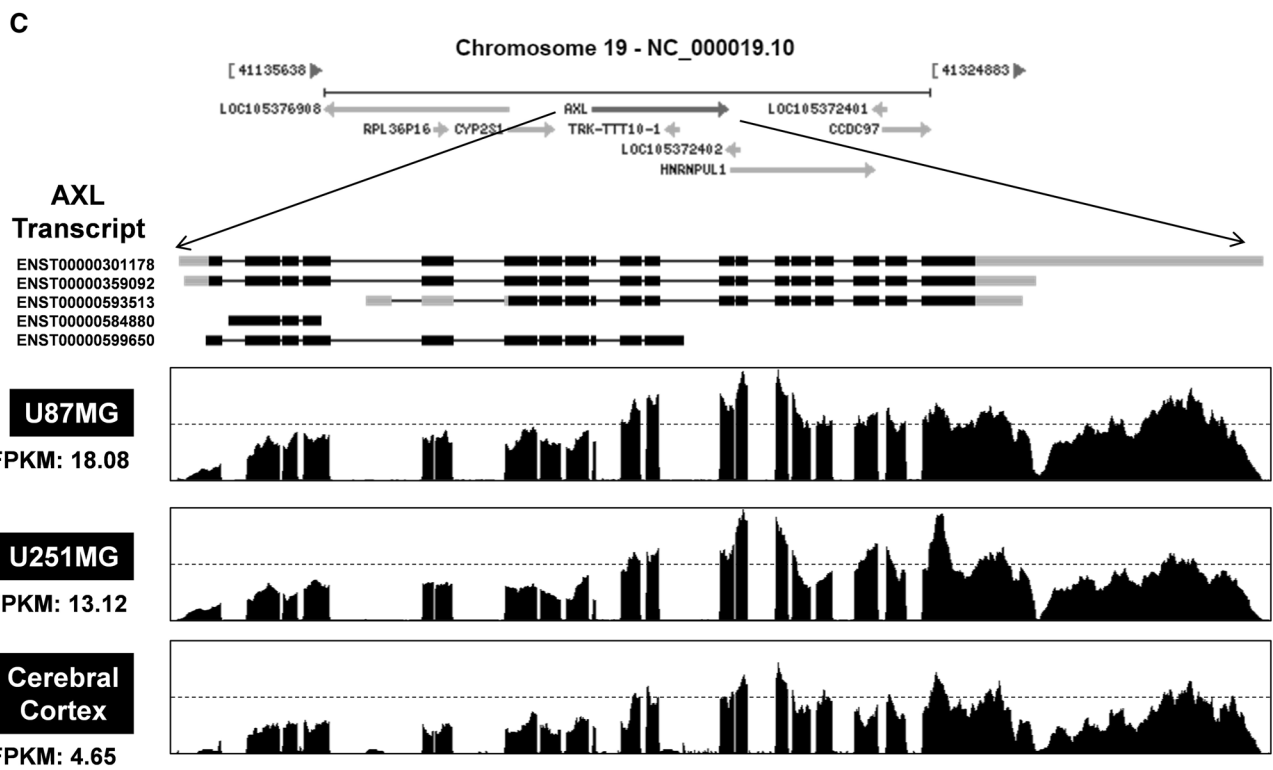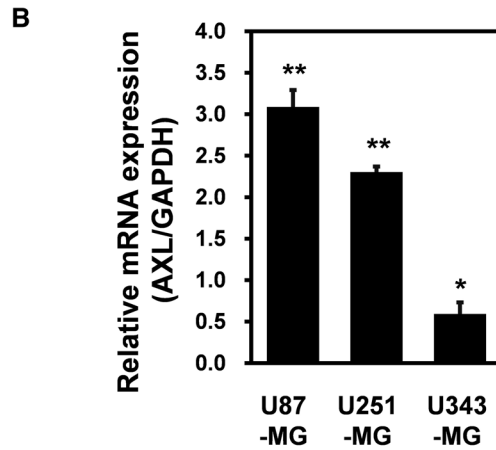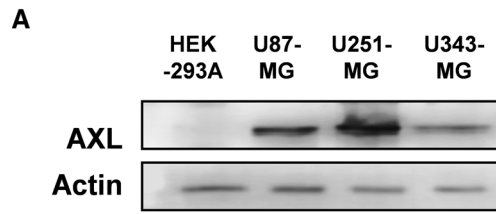
A

B

C

◄**Fig. 1** AXL expression in glioblastoma (GBM) cell lines. **a** Lysates were prepared from four established GBM cell lines (U87-MG, U251-MG and U373-MG) and subjected to western blotting using anti-AXL and anti-actin antibodies. The results are representative of three independent experiments (top panel). Relative densities were obtained by densitometry. Relative differences in AXL expression levels were calculated by normalizing all densitometric values to that of actin (in each lane). Results are presented as the means ± SDs of data from three independent experiments. **b** Total RNA extracted from each GBM cell line was analyzed by real-time quantitative reverse transcription-polymerase chain reaction (qRT-PCR) using human AXL-specific primers, as described in Materials and Methods. **C** Total RNAs were isolated from two GBM cell lines (U87-MG and U251-MG) and normal brain tissue. These samples were analyzed by standard RNA deep-sequencing (RNA-seq), as described in Materials and Methods. RNA-seq read densities of *AXL* transcripts were plotted against relative RNA-seq read coverages (counts). "Fragments per kilobase of exon per million fragments mapped" (FPKMs) were calculated to compare the expression levels of *AXL* mRNA variants among various samples. The results are presented as means ± SDs of data from three independent experiments. *$p < 0.05$, **$p < 0.01$

10 min. After washing twice with phosphate-buffered saline (PBS) for 5 min, two drops of Reagent A were added for blocking, and the slide was incubated for 30 min. Following two washes with PBS, the anti-AXL antibody was applied overnight at 4 °C. Then, biotinylated secondary antibody, Reagent B, was added after rinsing with PBS. The slide was incubated at room temperature for 1 h and then rinsed with PBS and mixed with enzyme-conjugated Reagent C. After washing with PBS, DAB chromogen, and a mixture of Reagent D1, D2, and D3, the reaction was stopped with distilled water, and pictures were taken with a microscope.

Bioinformatics data set

Human AXL expression in different tumor types from the TCGA database was analyzed at cBioPortal (http://www.cbioportal.org/index.do) based on 65,690 queried samples. The co-expression of AXL and HIF-1α was analyzed at cBioPortal based on 142 glioblastomas or 182 ovarian serous cystadenocarcinomata queried samples.

Statistical analysis

Data were expressed as the mean ± SD from at least three separate experiments. The differences between groups were analyzed using a Student's *t-test*, and $p < 0.05$ (*) was considered significant and $p < 0.01$ (**) was highly significant compared with corresponding control values. Statistical analyses were carried out using SPSS software ver. 13.0 (SPSS Inc.). For the analysis of the Kaplan–Meier survival curve, *P* values were obtained from the log-rank test, and the hazard ratio and 95% confidence interval were determined by a univariate Cox regression model.

Results

Upregulation of AXL expression in glioblastoma cell lines

To explore a putative role for AXL in brain cancer, western blotting using an anti-AXL antibody were performed. AXL expression was markedly enhanced in U87-MG and U251-MG GBM cells compared with other cells (Fig. 1A). Quantitative real-time PCR (qRT-PCR) of glioblastoma cell lines showed that the levels of mRNA encoding AXL were highly elevated in U87-MG cells (Fig. 1B). Based on the above observations, *AXL* mRNA levels were measured by RNA sequencing of glioblastoma cell lines. Total RNA was isolated from two cell lines (U87-MG and U251-MG), which showed high expression of AXL in Fig. 1A and B. We also isolated total RNA from normal brain cells. mRNAs were isolated from approximately 10 μg of total RNA, fragmented, and reverse-transcribed into cDNA. The numbers of "fragments per kilobase of exon per million fragments mapped" (FPKMs) were calculated to compare the expression levels of *AXL* mRNA among the various samples. As shown in Fig. 1C, the FPKMs were markedly higher in U87-MG cells (18.08) and U251-MG cells (13.12) than in cerebral cortex cells (4.65), indicating that AXL is transcriptionally upregulated in GBM cells.

Subcellular localization of AXL in U251-MG cells

The subcellular location of AXL in U251-MG cells was then determined by immunocytochemistry. AXL was found throughout the cytosolic area of the cell, including the tail-like cellular extensions or microvilli (Fig. 2). This suggested that AXL may play the important roles in cell migration, cell signaling and cell death.

AXL regulates cell migration and nutrient-dependent cell death in GBM

To determine if AXL affect cell migration or cell death, short-interfering RNA (siRNA) knockdown of AXL was employed. As shown in Fig. 3A, AXL reduction led to decreased the cell migration, which may be due to the function of microvilli-located AXL as shown in Fig. 2. Similarly, the cell viability in AXL knocking cells was also dramatically less than control cells (Fig. 3B). However, when the FBS was withdrawn, the cell viability indexes in the control and AXL-knockdown cells were similar (Fig. 3C), indicating that AXL-regulated cell death was dependent on the nutrient supply. Interestingly, FBS starvation decreased the expression of AXL, whereas epidermal growth factor (EGF) treatment did not (Fig. 3D). These results suggested that

Fig. 2 Subcellular localization of AXL in U251-MG cells U251-MG cells were grown on glass coverslips, fixed, and permeabilized with 0.2% (v/v) Triton X-100. After immunostaining with anti-AXL antibody, the coverslips were mounted on Vectashield and examined using a Zeiss confocal microscope. Scale bars: 10 μm
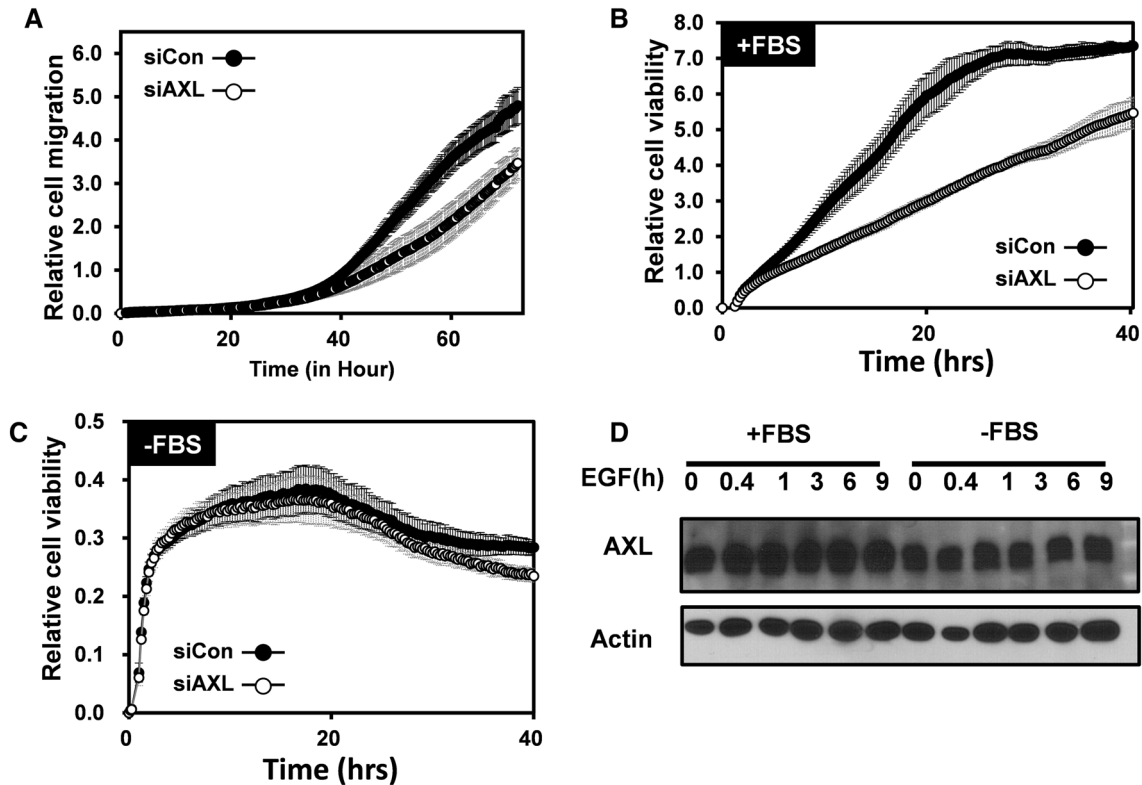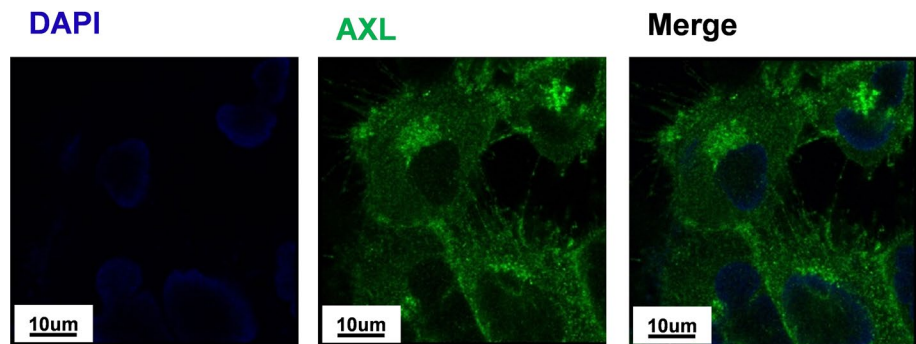

Fig. 3 AXL regulates cell migration and nutrient-dependent cell death in glioblastoma. **a** Real-time migration assay of U251-MG using the xCELLigence RTCA DP assay (n = 2) when cultured in fetal bovine serum (FBS)-containing media. The blue line indicates control siRNA-transfected cells, and the black circle indicates *AXL* siRNA-transfected cells. **b** Real-time proliferation assay of U251-MG using the xCELLigence RTCA DP assay (n = 2) when cultured in FBS-containing media. The white circle indicates the control siRNA-

transfected cells, and the black circle indicates the *AXL* siRNA-transfected cells. **c** Real-time proliferation assay of U251-MG using the xCELLigence RTCA DP assay (n = 2) when cultured in FBS-free media. White circle indicated for control siRNA transfected cells and red line indicated for *AXL* siRNA-transfected cells. **d** Immunoblot analysis with the indicated antibodies of lysates from U251-MG cells that were transfected with control siRNA or *AXL* siRNA under epidermal growth factor treatment condition

FBS regulated the AXL level, which affected the GBM cell viability.

AXL enhances the stabilization and nuclear translocation of HIF1α

AXL and HIF-1α were previously reported to be co-expressed in breast and renal cancer [37, 42]. Therefore, we

investigated the AXL-HIF-1α regulation. U251-MG cells were transfected with control siRNA or *AXL* siRNA before treatment with or without 150 μM $CoCl_2$ to mimic hypoxic conditions. Interestingly, HIF-1α stabilization was abolished when AXL was downregulated (Fig. 4A). This observation was further confirmed by immunocytochemistry analysis. However, *AXL* siRNA-transfected cells showed reduced levels of HIF-1α and prevented HIF-1α localization in the

Fig. 4 AXL regulates the stabilization and nuclear translocation of HIF-1α. **a** Immunoblot analysis with the indicated antibodies of lysates from U251-MG cells that were transfected with control siRNA or *AXL* siRNA under CoCl$_2$ treatment. **b** U251-MG cells were grown on glass coverslips and transfected with control siRNA or *AXL* siRNA. Next, the cells were treated with or without 150 μM CoCl$_2$ for 24 h, fixed, and permeabilized with 0.2% (v/v) Triton X-100. After immunostaining with anti-HIF1 antibody, the coverslips were mounted on Vectashield and examined using a Zeiss confocal microscope. Scale bars: 20 μm. **c** U251-MG cells were grown on glass coverslips and treated with or without 150 μM CoCl$_2$ for 24 h. The cells were then fixed and permeabilized with 0.2% (v/v) Triton X-100. After immunostaining with anti-AXL antibody, the coverslips were mounted on Vectashield and examined using a Zeiss confocal microscope. Scale bars: 20 μm
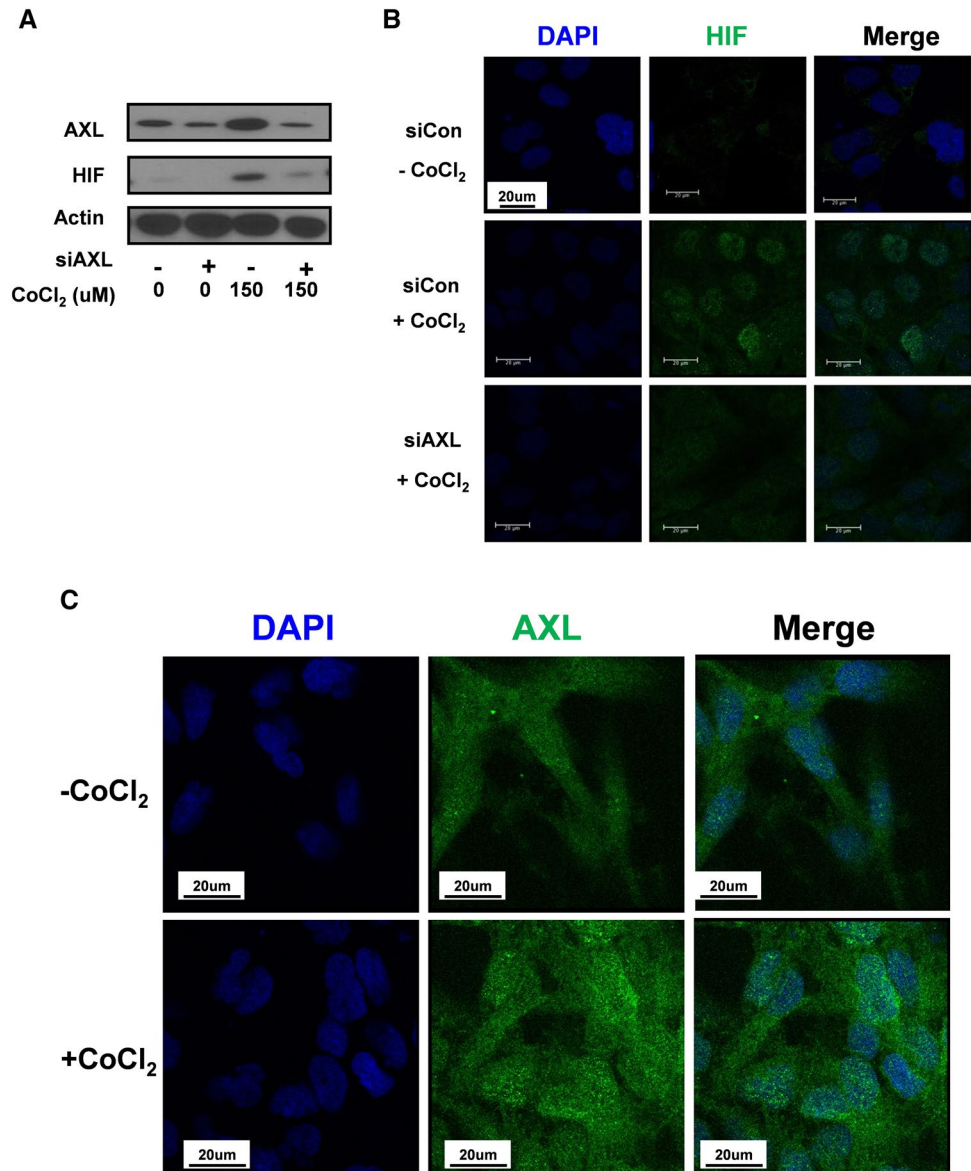
nucleus, even in cells that were also treated with CoCl$_2$ (Fig. 4B). Hence, AXL played an important role in the stabilization and nuclear translocation of HIF-1α under hypoxic conditions. Surprisingly, CoCl$_2$ treatment also induced AXL expression as well as nuclear-located AXL (Fig. 4C), suggesting AXL stabilized HIF-1α under hypoxic conditions.

Co-expression of AXL and HIF-1α in glioblastomas from patients

To validate whether AXL plays a pivotal role in human cancer, we investigated *AXL* mRNA expression in multiple malignancies. RNA-sequencing data from The Cancer Genome Atlas

(TCGA) showed that *AXL* mRNA expression is upregulated in most cancer types, including GBM and glioma (Fig. 5A). To confirm further the above observations in clinical samples, immunohistochemical (IHC) analysis with the human cancer tissue array was used. IHC analysis with an anti-AXL antibody showed a strong signal in tumor tissue, as compared to surrounding normal tissues (Fig. 5B). As expected, HIF-1α also showed a higher signal in GBM (Fig. 5C). Moreover, by analyzing 142 Glioblastoma samples at http://www.cbioportal.org, we found that the exposure of the Pearson's correlation index was 0.36, which indicated a weak uphill linear relationship between *AXL* and *HIF-1α* mRNA levels (Fig. 5D). Interestingly, this correlation was absent in cases of ovarian serous

A

F

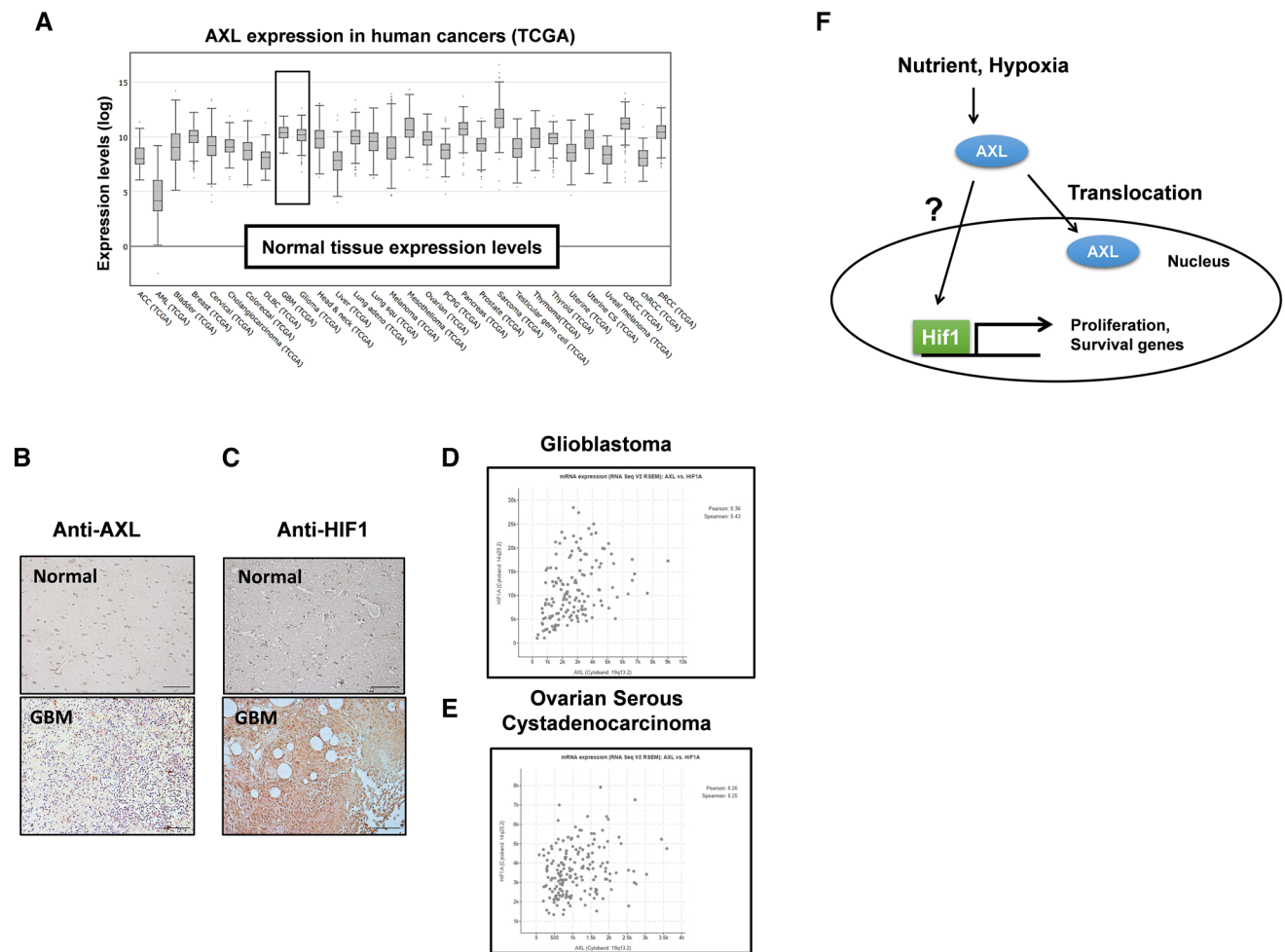**B**   **C**   **D**   **E**

Fig. 5 The expression of AXL and HIF-1α in human glioma. **a** Human AXL expression in different tumor types from the TCGA database. Adapted from cBioPortal: http://www.cbioportal.org/index.do. **b** Human glioma tissue arrays were immuno-histochemically analyzed in terms of AXL staining. Representative images from samples from two patients are shown. Scale bars: 100 μm. **c** Human glioma tissue arrays were immunohistochemically analyzed in terms of HIF-1α staining. Representative images from samples from two patients are shown. Scale bars: 100 μm. **d** the co-expression of *AXL* mRNA and *HIF-1α* mRNA from 142 queried glioblastoma (GBM) samples in the TCGA database. **e** The co-expression of *AXL* mRNA and *HIF-1α* mRNA from 182 ovarian serous cystadenocarcinoma queried samples. Adapted from cBioPortal: http://www.cbioportal.org/index.do. **f** The working model of the role of AXL in GBM survival. Under the control of the tumor microenvironment, such as the nutrient supply and hypoxia conditions, AXL translocates to the nucleus. The inhibition of HIF-1α degradation and the nuclear trans-localization of HIF-1α by hypoxia trigger the expression of AXL. Nuclear HIF-1α promotes the proliferation and survival genes in GBM

cystadenocarcinoma, which showed a Pearson's correlation inde× of 0.26 (Fig. 5E). These results supported the role of AXL-HIF-1α association in GBM development.

Discussion

GBM is the most aggressive type of central nervous system (CNS) tumor. The prognosis of GBM is poor even when multiple therapies are applied [43]. Molecular targeting may be important when developing efficient GBM treatment strategies. In 2016, WHO changed the CNS tumor classification to a molecular categorization based on genetic and epigenetic features, which was based on histopathological criteria established in the 1920s developed by Bailey and Cushing [44]. Therefore, prognostic biomarkers and potential molecular targets must be identified to improve the prognosis of GBM. In the present study, we showed that AXL is a novel GBM prognostic marker in the GBM cell line and in patient tissue (Fig. 1, 5A and B), which supported previous studies [8–10]. Remarkably, AXL is a member of the RTK/RAS/PI3K pathway, which was altered in 88% of GBM samples [6, 7]. We also showed that AXL knockdown reduced growth and cell migration in the GBM U251MG cell line (Fig. 3A and B). Interestingly, AXL knockdown decreased the viability

of U251MG cells cultured in FBS-containing media but not in FBS-free media, indicating that AXL-related cell viability is nutrient-dependent (Fig. 3C). Moreover, serum starvation decreased the viability index to 0.4 at 20 h (Fig. 3C) compared to 5.0 when the cells were cultured in FBS-containing media. Previous studies have shown that activation of the EGFR pathway and downstream MEK/ERK signaling can upregulate AXL mRNA expression through the JUN transcription factor in non-small-cell lung cancer and head and neck squamous cell carcinoma [45]. However, in our study, we did not observe any effect of EGF on the expression of AXL. Although the impact of nutrient supply on AXL expression was inconsistent, we found that serum starvation also reduced the level of AXL (Fig. 3D), suggesting that AXL is a potential mediator in serum-regulated GBM cell growth.

The relation of nutrient/PKB/HIF-1α to tumor growth is well known in a recent study, AXL was found to be a key upstream effector of PKB [46], indicating a relationship between AXL and HIF-1α modulation. Indeed, the expression of HIF-1α and AXL were both upregulated in a GBM patient sample (Fig. 5B and C), consistent with a previous study [46]. Moreover, analysis from TCGA indicated that AXL was positively co-regulated with HIF-1α in GBM (Fig. 5D) but not in ovarian serous cystadenocarcinoma (Fig. 5E). Our study provides evidence that AXL plays a crucial role in regulating the stabilization and nuclear localization of HIF-1α in GBM (Fig. 4A and B), both of which are essential for cancer development and implicated in tumor growth [29]. Notably, our findings show that AXL levels and localization are also affected by hypoxia-mimicking conditions, as seen with the treatment of CoCl2 in prostate cancer [47]. Specifically, we observed that AXL is present in the cytosol and microvilli, suggesting its potential involvement in cell migration and signaling pathways that may impact microvilli and ER functions [48, 49]. Interestingly, our study revealed that CoCl2 treatment increases nuclear AXL levels, indicating a possible regulatory role of CoCl2 in AXL's nuclear translocation. Further investigation is warranted to better understand the molecular mechanisms underlying these observations.

Overall, this study contributed to the understanding of AXL-remodeling GBM growth and migration, which could be a potential therapeutic strategy in GBM treatment.

Declarations

Conflict of interest The authors declare that they have no competing interests.

References

1. Ostrom QT, Bauchet L, Davis FG, Deltour I, Fisher JL, Langer CE, Pekmezci M, Schwartzbaum JA, Turner MC, Walsh KM, Wrensch MR, Barnholtz-Sloan JS (2014) The epidemiology of glioma in adults: a "state of the science" review. Neuro Oncol 16:896–913. https://doi.org/10.1093/neuonc/nou087

2. Ostrom QT, Cote DJ, Ascha M, Kruchko C, Barnholtz-Sloan JS (2018) Adult glioma incidence and survival by race or ethnicity in the united states from 2000 to 2014. JAMA Oncol 4:1254–1262. https://doi.org/10.1001/jamaoncol.2018.1789

3. Louis DN, Perry A, Wesseling P, Brat DJ, Cree IA, Figarella-Branger D, Hawkins C, Ng HK, Pfister SM, Reifenberger G, Soffietti R, von Deimling A, Ellison DW (2021) The 2021 WHO classification of tumors of the central nervous system: a summary. Neuro Oncol 23:1231–1251. https://doi.org/10.1093/neuonc/noab106

4. Zakharova G, Efimov V, Raevskiy M, Rumiantsev P, Gudkov A, Belogurova-Ovchinnikova O, Sorokin M, Buzdin A (2022) Reclassification of TCGA diffuse glioma profiles linked to transcriptomic, epigenetic, genomic and clinical data, according to the 2021 WHO CNS tumor classification. Int J Mol Sci 24:157. https://doi.org/10.3390/ijms24010157

5. Mohammed S, Dinesan M, Ajayakumar T (2022) Survival and quality of life analysis in glioblastoma multiforme with adjuvant chemoradiotherapy: a retrospective study. Rep Pract Oncol Radiother 27:1026–1036. https://doi.org/10.5603/RPOR.a2022.0113

6. Brennan CW, Verhaak RG, McKenna A, Campos B, Noushmehr H, Salama SR, Zheng S, Chakravarty D, Sanborn JZ, Berman SH, Beroukhim R, Bernard B, Wu CJ, Genovese G, Shmulevich I, Barnholtz-Sloan J, Zou L, Vegesna R, Shukla SA, Ciriello G, Yung WK, Zhang W, Sougnez C, Mikkelsen T, Aldape K, Bigner DD, Van Meir EG, Prados M, Sloan A, Black KL, Eschbacher J, Finocchiaro G, Friedman W, Andrews DW, Guha A, Iacocca M, O'Neill BP, Foltz G, Myers J, Weisenberger DJ, Penny R, Kucherlapati R, Perou CM, Hayes DN, Gibbs R, Marra M, Mills GB, Lander E, Spellman P, Wilson R, Sander C, Weinstein J, Meyerson M, Gabriel S, Laird PW, Haussler D, Getz G, Chin L,

Network TR (2013) The somatic genomic landscape of glioblastoma. Cell 155:462–477. https://doi.org/10.1016/j.cell.2013.09.034

7. Verhaak RG, Hoadley KA, Purdom E, Wang V, Qi Y, Wilkerson MD, Miller CR, Ding L, Golub T, Mesirov JP, Alexe G, Lawrence M, O'Kelly M, Tamayo P, Weir BA, Gabriel S, Winckler W, Gupta S, Jakkula L, Feiler HS, Hodgson JG, James CD, Sarkaria JN, Brennan C, Kahn A, Spellman PT, Wilson RK, Speed TP, Gray JW, Meyerson M, Getz G, Perou CM, Hayes DN, Cancer Genome Atlas Research N (2010) Integrated genomic analysis identifies clinically relevant subtypes of glioblastoma characterized by abnormalities in PDGFRA, IDH1, EGFR, and NF1. Cancer Cell 17:98–110. https://doi.org/10.1016/j.ccr.2009.12.020

8. Li Y, Ye X, Tan C, Hongo JA, Zha J, Liu J, Kallop D, Ludlam MJ, Pei L (2009) Axl as a potential therapeutic target in cancer: role of Axl in tumor growth, metastasis and angiogenesis. Oncogene 28:3442–3455. https://doi.org/10.1038/onc.2009.212

9. Hutterer M, Knyazev P, Abate A, Reschke M, Maier H, Stefanova N, Knyazeva T, Barbieri V, Reindl M, Muigg A, Kostron H, Stockhammer G, Ullrich A (2008) Axl and growth arrest-specific gene 6 are frequently overexpressed in human gliomas and predict poor prognosis in patients with glioblastoma multiforme. Clin Cancer Res 14:130–138. https://doi.org/10.1158/1078-0432.CCR-07-0862

10. Onken J, Torka R, Korsing S, Radke J, Krementeskaia I, Nieminen M, Bai X, Ullrich A, Heppner F, Vajkoczy P (2016) Inhibiting receptor tyrosine kinase AXL with small molecule inhibitor BMS-777607 reduces glioblastoma growth, migration, and invasion in vitro and in vivo. Oncotarget 7:9876–9889. https://doi.org/10.18632/oncotarget.7130

11. O'Bryan JP, Frye RA, Cogswell PC, Neubauer A, Kitch B, Prokop C, Espinosa R 3rd, Le Beau MM, Earp HS, Liu ET (1991) AXL, a transforming gene isolated from primary human myeloid leukemia cells, encodes a novel receptor tyrosine kinase. Mol Cell Biol 11:5016–5031. https://doi.org/10.1128/mcb.11.10.5016-5031.1991

12. Craven RJ, Xu LH, Weiner TM, Fridell YW, Dent GA, Srivastava S, Varnum B, Liu ET, Cance WG (1995) Receptor tyrosine kinases expressed in metastatic colon cancer. Int J Cancer 60:791–797. https://doi.org/10.1002/ijc.2910600611

13. Ito T, Ito M, Naito S, Ohtsuru A, Nagayama Y, Kanematsu T, Yamashita S, Sekine I (1999) Expression of the AXL receptor tyrosine kinase in human thyroid carcinoma. Thyroid 9:563–567. https://doi.org/10.1089/thy.1999.9.563

14. Berclaz G, Altermatt HJ, Rohrbach V, Kieffer I, Dreher E, Andres AC (2001) Estrogen dependent expression of the receptor tyrosine kinase AXL in normal and malignant human breast. Ann Oncol 12:819–824. https://doi.org/10.1023/a:1011126330233

15. Sun W, Fujimoto J, Tamaya T (2004) Coexpression of Gas6/AXL in human ovarian cancers. Oncology 66:450–457. https://doi.org/10.1159/000079499

16. Shieh YS, Lai CY, Kao YR, Shiah SG, Chu YW, Lee HS, Wu CW (2005) Expression of AXL in lung adenocarcinoma and correlation with tumor progression. Neoplasia 7:1058–1064. https://doi.org/10.1593/neo.05640

17. Giles KM, Kalinowski FC, Candy PA, Epis MR, Zhang PM, Redfern AD, Stuart LM, Goodall GJ, Leedman PJ (2013) AXL mediates acquired resistance of head and neck cancer cells to the epidermal growth factor receptor inhibitor erlotinib. Mol Cancer Ther 12:2541–2558. https://doi.org/10.1158/1535-7163.MCT-13-0170

18. Sainaghi PP, Castello L, Bergamasco L, Galletti M, Bellosta P, Avanzi GC (2005) Gas6 induces proliferation in prostate carcinoma cell lines expressing the AXL receptor. J Cell Physiol 204:36–44. https://doi.org/10.1002/jcp.20265

19. Falcone I, Conciatori F, Bazzichetto C, Bria E, Carbognin L, Malaguti P, Ferretti G, Cognetti F, Milella M, Ciuffreda L (2020) AXL receptor in breast cancer: molecular involvement and therapeutic limitations. Int J Mol Sci 21. https://doi.org/10.3390/ijms21228419

20. He L, Lei Y, Hou J, Wu J and Lv G (2020) Implications of the receptor tyrosine kinase Axl in gastric cancer progression. Onco Targets Ther 13:5901–5911. https://doi.org/10.2147/ott.S257606

21. Chung BI, Malkowicz SB, Nguyen TB, Libertino JA, McGarvey TW (2003) Expression of the proto-oncogene AXL in renal cell carcinoma. DNA Cell Biol 22:533–540. https://doi.org/10.1089/10445490360708946

22. Mahadevan D, Cooke L, Riley C, Swart R, Simons B, Della Croce K, Wisner L, Iorio M, Shakalya K, Garewal H, Nagle R, Bearss D (2007) A novel tyrosine kinase switch is a mechanism of imatinib resistance in gastrointestinal stromal tumors. Oncogene 26:3909–3919. https://doi.org/10.1038/sj.onc.1210173

23. Hong CC, Lay JD, Huang JS, Cheng AL, Tang JL, Lin MT, Lai GM, Chuang SE (2008) Receptor tyrosine kinase AXL is induced by chemotherapy drugs and overexpression of AXL confers drug resistance in acute myeloid leukemia. Cancer Lett 268:314–324. https://doi.org/10.1016/j.canlet.2008.04.017

24. Stone L (2017) Kidney cancer: AXL expression predicts prognosis. Nat Rev Urol 14:700. https://doi.org/10.1038/nrurol.2017.186

25. Ghiso E, Migliore C, Ciciriello V, Morando E, Petrelli A, Corso S, De Luca E, Gatti G, Volante M, Giordano S (2017) YAP-dependent AXL overexpression mediates resistance to EGFR inhibitors in NSCLC. Neoplasia 19:1012–1021. https://doi.org/10.1016/j.neo.2017.10.003

26. Kanlikilicer P, Ozpolat B, Aslan B, Bayraktar R, Gurbuz N, Rodriguez-Aguayo C, Bayraktar E, Denizli M, Gonzalez-Villasana V, Ivan C, Lokesh GLR, Amero P, Catuogno S, Haemmerle M, Wu SY, Mitra R, Gorenstein DG, Volk DE, de Franciscis V, Sood AK and Lopez-Berestein G (2017) Therapeutic targeting of AXL receptor tyrosine kinase inhibits tumor growth and intraperitoneal metastasis in ovarian cancer models. Mol Ther Nucleic Acids 9:251–262. https://doi.org/10.1016/j.omtn.2017.06.023

27. Bao B, Azmi AS, Ali S, Ahmad A, Li Y, Banerjee S, Kong D, Sarkar FH (2012) The biological kinship of hypoxia with CSC and EMT and their relationship with deregulated expression of miRNAs and tumor aggressiveness. Biochim Biophys Acta 1826:272–296. https://doi.org/10.1016/j.bbcan.2012.04.008

28. Masoud GN, Li W (2015) HIF-1α pathway: role, regulation and intervention for cancer therapy. Acta Pharm Sin B 5:378–389. https://doi.org/10.1016/j.apsb.2015.05.007

29. Liu ZJ, Semenza GL, Zhang HF (2015) Hypoxia-inducible factor 1 and breast cancer metastasis. J Zhejiang Univ Sci B 16:32–43. https://doi.org/10.1631/jzus.B1400221

30. Forsythe JA, Jiang BH, Iyer NV, Agani F, Leung SW, Koos RD, Semenza GL (1996) Activation of vascular endothelial growth factor gene transcription by hypoxia-inducible factor 1. Mol Cell Biol 16:4604–4613. https://doi.org/10.1128/MCB.16.9.4604

31. Hanahan D, Weinberg RA (2000) The hallmarks of cancer. Cell 100:57–70. https://doi.org/10.1016/s0092-8674(00)81683-9

32. Hanahan D, Folkman J (1996) Patterns and emerging mechanisms of the angiogenic switch during tumorigenesis. Cell 86:353–364. https://doi.org/10.1016/S0092-8674(00)80108-7

33. Skobe M, Rockwell P, Goldstein N, Vosseler S, Fusenig NE (1997) Halting angiogenesis suppresses carcinoma cell invasion. Nat Med 3:1222–1227. https://doi.org/10.1038/nm1197-1222

34. Nalwoga H, Ahmed L, Arnes JB, Wabinga H, Akslen LA (2016) Strong expression of hypoxia-inducible factor-1α (HIF-1α) is associated with AXL expression and features of aggressive tumors in African breast cancer. PLoS One 11:e0146823. https://doi.org/10.1371/journal.pone.0146823

35. Goyette MA, Elkholi IE, Apcher C, Kuasne H, Rothlin CV, Muller WJ, Richard DE, Park M, Gratton JP, Côté JF (2021) Targeting AXL favors an antitumorigenic microenvironment that enhances immunotherapy responses by decreasing Hif-1α levels. Proc Natl Acad Sci USA 118:e2023868118. https://doi.org/10.1073/pnas.2023868118

36. Raval RR, Lau KW, Tran MG, Sowter HM, Mandriota SJ, Li JL, Pugh CW, Maxwell PH, Harris AL, Ratcliffe PJ (2005) Contrasting properties of hypoxia-inducible factor 1 (HIF-1) and HIF-2 in von Hippel-Lindau-associated renal cell carcinoma. Mol Cell Biol 25:5675–5686. https://doi.org/10.1128/mcb.25.13.5675-5686.2005

37. Shen C, Beroukhim R, Schumacher SE, Zhou J, Chang M, Signoretti S, Kaelin WG Jr (2011) Genetic and functional studies implicate HIF1α as a 14q kidney cancer suppressor gene. Cancer Discov 1:222–235. https://doi.org/10.1158/2159-8290.cd-11-0098

38. Mazumder S, Higgins PJ, Samarakoon R (2023) Downstream targets of VHL/HIF-α signaling in renal clear cell carcinoma progression: mechanisms and therapeutic relevance. Cancers (Basel) 15:1316. https://doi.org/10.3390/cancers15041316

39. Na AY, Yang EJ, Jeon JM, Ki SH, Song KS, Lee S (2018) Protective effect of isoliquiritigenin against ethanol-induced hepatic steatosis by regulating the SIRT1-AMPK pathway. Toxicol Res 34:23–29. https://doi.org/10.5487/TR.2018.34.1.023

40. Tran Q, Jung JH, Park J, Lee H, Hong Y, Cho H, Kim M, Park S, Kwon SH, Kim SH, Thomas G, Kim KP, Cho MH, Park J (2018) S6 kinase 1 plays a key role in mitochondrial morphology and cellular energy flow. Cell Signal 48:13–24. https://doi.org/10.1016/j.cellsig.2018.04.002

41. Na CH, Hong JH, Kim WS, Shanta SR, Bang JY, Park D, Kim HK, Kim KP (2015) Identification of protein markers specific for papillary renal cell carcinoma using imaging mass spectrometry. Mol Cells 38:624–629. https://doi.org/10.14348/molcells.2015.0013

42. Nalwoga H, Ahmed L, Arnes JB, Wabinga H, Akslen LA (2016) Strong expression of hypoxia-inducible factor-1alpha (HIF-1alpha) is associated with AXL expression and features of aggressive tumors in African breast cancer. PLoS One 11:e0146823. https://doi.org/10.1371/journal.pone.0146823

43. Fernandes G, Fernandes BC, Valente V, Dos Santos JL (2018) Recent advances in the discovery of small molecules targeting glioblastoma. Eur J Med Chem 164:8–26. https://doi.org/10.1016/j.ejmech.2018.12.033

44. Geraldo LHM, Garcia C, da Fonseca ACC, Dubois LGF, de Sampaio ESTCL, Matias D, de Camargo Magalhaes ES, do Amaral RF, da Rosa BG, Grimaldi I, Leser FS, Janeiro JM, Macharia L, Wanjiru C, Pereira CM, Moura-Neto V, Freitas C, Lima FRS (2019) Glioblastoma therapy in the age of molecular medicine. Trends Cancer 5:46–65. https://doi.org/10.1016/j.trecan.2018.11.002

45. Brand TM, Iida M, Stein AP, Corrigan KL, Braverman CM, Luthar N, Toulany M, Gill PS, Salgia R, Kimple RJ, Wheeler DL (2014) AXL mediates resistance to cetuximab therapy. Cancer Res 74:5152–5164. https://doi.org/10.1158/0008-5472.Can-14-0294

46. Zuo Q, Liu J, Huang L, Qin Y, Hawley T, Seo C, Merlino G, Yu Y (2018) AXL/AKT axis mediated-resistance to BRAF inhibitor depends on PTEN status in melanoma. Oncogene 37:3275–3289. https://doi.org/10.1038/s41388-018-0205-4

47. Mishra A, Wang J, Shiozawa Y, McGee S, Kim J, Jung Y, Joseph J, Berry JE, Havens A, Pienta KJ, Taichman RS (2012) Hypoxia stabilizes GAS6/AXL signaling in metastatic prostate cancer. Mol Cancer Res 10:703–712. https://doi.org/10.1158/1541-7786.MCR-11-0569

48. Mattila PK, Lappalainen P (2008) Filopodia: molecular architecture and cellular functions. Nat Rev Mol Cell Biol 9:446–454. https://doi.org/10.1038/nrm2406

49. Obacz J, Avril T, Le Reste PJ, Urra H, Quillien V, Hetz C, Chevet E (2017) Endoplasmic reticulum proteostasis in glioblastoma-from molecular mechanisms to therapeutic perspectives. Sci Signal 10:eaal2323. https://doi.org/10.1126/scisignal.aal2323